



## A Characteristic-based Solution of Forced and Free Convection in Closed Domains with Emphasis on Various Fluids

T. Adibi<sup>\*a</sup>, O. Adibi<sup>b</sup>, S. E. Razavi<sup>c</sup>

<sup>a</sup> Department of Mechanical Engineering, University of Bonab, Bonab, Iran

<sup>b</sup> Department of Mechanical Engineering, Sharif University of Technology, Tehran, Iran

<sup>c</sup> Department of Mechanical Engineering, University of Tabriz, Tabriz, Iran

### PAPER INFO

#### Paper history:

Received 23 August 2019

Received in revised form 12 September 2019

Accepted 13 September 2019

#### Keywords:

complex boundary conditions  
convection

Grashof number

numerical method

Nusselt number

Prandtl number

### ABSTRACT

In this paper, forced and free convection in the cavity is simulated numerically with complex boundary conditions. Temperature changes sinusoidally at the upper and right walls and the temperature of the other walls is kept at zero. The effects of Prandtl and Grashof numbers variations on flow patterns are surveyed. A wide range of materials, e.g. molten metals, gases, water, and coolant liquid are considered. For this purpose, an in-house code is written in FORTRAN-95 within the finite volume framework. For time discretization, the fifth-order Rung-Kutta method is applied. The convective terms are calculated by a novel characteristic-based scheme along with artificial compressibility. The flow is assumed to be incompressible, laminar and two dimensional. It was found that higher Nusselt numbers have affected increasing Grashof numbers. The effect of Gr on Nu at the upper wall is stronger than that of the down wall. However, the effect of Pr on Nu at upper wall is almost equal with that of the down wall.

doi: 10.5829/ije.2019.32.11b.20

### NOMENCLATURE

2D	Two-dimensional	T	Temperature
D	Damping	t	Time
g	Gravitational acceleration	u, v, w	X, y, z velocity components
Gr	Grashof number	x, y, z	Coordinates
k	Thermal conductivity	ref	Reference
M	Number of cells in x-direction	<b>Greek Symbols</b>	
N	Number of cells in y-direction	$\beta$	Artificial compressibility coefficient
Nu	Local Nusselt number	$\beta_{ex}$	Thermal expansion coefficient
$\overline{Nu}$	Mean Nusselt number	$\varepsilon$	Damping coefficient
p	Pressure	$\mu$	Coefficient of viscosity
Pr	Prandtl number	$\nu$	Kinematic viscosity
Re	Reynolds number	$\rho$	Density

## 1. INTRODUCTION

Heat transfer happens in various industries. The industrial applications of this study are solar collectors, thermal building, electronic cooling, aeronautics, and chemical apparatus. Therefore, it is important that Heat transfer rate be calculated. The first and the cheapest

method is of solving governing equations analytically. However, in most cases, there are no analytical solutions for the governing equations. The second method is the experimental method. Experimental methods are very expensive. The other alternative is numerical method. The researchers in recent decades have numerically solved the governing equations under different boundary

\*Corresponding Author Email: tohidadibi@bonabu.ac.ir.(T. Adibi)

conditions. Moallemi and Jang [1] solved mixed convection for cavity flow. The influence of Prandtl number on flow characteristics is surveyed. Laminar incompressible flow is simulated. Oztop and Dagtekin [2] numerically simulated steady state two-dimensional mixed convection problem in a vertical two-sided lid-driven differentially heated square cavity. The left and right moving walls were maintained at different constant temperatures while upper and bottom walls were thermally insulated. Sharif [3] numerically solved laminar mixed convective heat transfer in two-dimensional shallow rectangular driven cavities of aspect ratio 10. The Rayleigh numbers varies between  $10^5$  and  $10^7$  and the Reynolds Prandtl numbers fixed at 408.21 and 6, respectively. Adibi and Razavi [4, 5] in two different works, simulated natural and forced convection in few bench marks including flow in a square cavity by their own proposed scheme. Their method is compared with averaging scheme. Christopher [6] numerically solved the equations for natural convection flow in a tall cavity. The objective was to compare various solution methods for this complex flow situation. Refaee et al. [7] numerically simulated two-dimensional natural convection in a partially cooled, differentially heated inclined cavities. Padilla et al. [8] numerically simulated three dimensional natural convection. Two walls of a cubic are considered at different temperatures and the other four are adiabatic. Finite volume method is used in their works. Selimefendigil [9] numerically simulated two dimensional laminar flow in a cavity. Navier- Stokes equations are solved and streamlines and isotherms are obtained. Labsi et al. [10] studied two dimensional cavity flow with heat transfer numerically. The upper and the bottom walls are adiabatic and the other ones are heated. Finite volume method is used. Bousset et al. [11] numerically simulated three dimensional convection in cavity flow. Simulations have been done for different Prandtl numbers. Gershuni et al. [12] studied two dimensional convection in cavity flow numerically. The different characteristics of the above-mentioned simulation is reported in this work. Alonso and Batiste [13] work on the convection flow in cavity and the influence of the transverse walls on the onset of convection is surveyed. The down wall of the cavity is heated in this work. Boeck [14] simulated convection flow in cavity in low Prandtl number in two and three dimensions. The effect of a magnetic field on flow pattern was surveyed in this work. Jami et al. [15] did a numerical investigation of the laminar-free convective heat transfer in a square enclosure containing a solid cylinder located at an arbitrary position. Effects of the cylinder position on heat transfer and flow structures inside the cavity are to be surveyed. Armfield and Schultz [16] numerically solved natural convection in cavity. QUICK scheme is used. Raji and Hasnaoui [17] numerically simulated mixed convection and thermal

radiation in ventilated cavities with gray surfaces using the Navier-Stokes equations with the Boussinesq approximation. Mukherjee et al. [18] numerically investigated on incompressible Newtonian viscous flow. Different boundary conditions are considered and Nusselt number is obtained in different conditions. Nassab et al. [19] numerically studied conductive and radiative heat transfer. Finite volume method was used. Reyhani et al. [20] numerically studied heat transfer. Finite volume and finite element methods were used in triangle grids. In this work, a code is written in FORTRAN software to simulate heat transfer in different Grashof, Reynolds, and Prandtl numbers. Streamlines, isotherms, temperatures and velocities in centerlines of cavity, Nusselt number and mean Nusselt number are obtained in this work. Also, the procedure of numerical method is explained in details. Forced and free convection are simulated under various conditions in this work due to their importance. In comparison to the preceding studies, the originality of this paper is the difference in the applied scheme and complex boundary conditions. Also, in this work simulations are done for a wide range of Reynolds, Prandtl, and Grashof numbers. Some practical and industrial problems of this work may include the effect of free-convection on cooling of dye-cast materials. In this paper, a characteristic method introduced by us before is adopted for convective fluxes. In previous works, very simple boundary conditions have been used however; in practice, the boundary conditions are not so simple. Changing the boundary conditions in some cases could add more complication in numerical solutions.

## 2. GOVERNING EQUATIONS

The governing equations for the two-dimensional (2D) incompressible viscous flow with heat transfer in dimensionless form are [21]

$$\begin{aligned} \frac{1}{\beta} \frac{\partial p}{\partial t} + \frac{\partial u}{\partial x} + \frac{\partial v}{\partial y} &= 0; \quad \frac{\partial u}{\partial t} + u \frac{\partial u}{\partial x} + v \frac{\partial u}{\partial y} = -\frac{\partial p}{\partial x} + \\ \frac{1}{Re} \frac{\partial^2 u}{\partial x^2} + \frac{\partial v}{\partial y^2} + u \frac{\partial v}{\partial x} + v \frac{\partial v}{\partial y} &= -\frac{Gr}{Re^2} T - \frac{\partial p}{\partial y} + \\ \frac{1}{Re} \frac{\partial^2 v}{\partial x^2} + \frac{\partial T}{\partial t} + u \frac{\partial T}{\partial x} + v \frac{\partial T}{\partial y} &= Ec \left( u \frac{\partial p}{\partial x} + v \frac{\partial p}{\partial y} \right) + \\ \frac{1}{RePr} \frac{\partial^2 T}{\partial x^2} + \frac{\partial^2 T}{\partial y^2} & \end{aligned} \quad (1)$$

In the above equations, the first equation is the continuity equation, the second and the third ones are momentum equations and the last one is the energy equation. In the free and the mixed convection, density is not constant. Therefore, the Boussinesq assumption is used in the y-momentum equation. Also, the artificial compressibility is applied in this paper in continuity equation. Equation (2) is used to transfer Navier-Stokes equation to dimensionless form (Equation (1)).

$$u^* = \frac{u}{U_{ref}}, v^* = \frac{v}{U_{ref}}, x^* = \frac{x}{L_{ref}}, y^* = \frac{y}{L_{ref}}, p^* = \frac{p + \rho g y - p_o}{\rho_{ref} U_{ref}^2}, t^* = \frac{t U_{ref}}{L_{ref}}, T^* = \frac{T - T_{ref1}}{T_{ref2} - T_{ref1}} \quad (2)$$

where  $U_{ref}$  is the reference velocity,  $L_{ref}$  the reference length,  $T_{ref1}$  the first reference temperature and  $T_{ref2}$  the second reference temperature. These references depend on the numerical problem. For cavity flow  $U_{ref}$  is the velocity of the upper surface,  $L_{ref}$  is the length of the cavity,  $T_{ref1}$  and  $T_{ref2}$  are the maximum and the minimum walls temperatures. In Equation (1), the stars are omitted and Re, Pr, Ec, and Gr are defined as:

$$Re = \frac{\rho_{ref} U_{ref} L_{ref}}{\mu}, Pr = \frac{c_p \mu}{k}, Ec = \frac{u_{ref}^2}{c_p (T_{ref2} - T_{ref1})}, Gr = \frac{\beta_{ex} g (T_{ref2} - T_{ref1}) L_{ref}^3}{\nu^2} \quad (3)$$

where Re, Gr, Pr and Ec are the Reynolds, Grashof, Prandtl, and Eckert numbers, respectively. After some mathematical calculations and using the Green theorem, the governing equations for the 2D incompressible viscous thermo-flow in the finite-volume form can be expressed as:

$$\frac{\partial}{\partial t} \iint Q dA + \oint ((F - R) dy - (G - S) dx) = \iint H dA, \quad (4)$$

In the above equations ‘F’ and ‘G’ denote the convective fluxes and ‘R’ and ‘S’ are the viscous fluxes and ‘H’ is source term.

### 3. NUMERICAL PROCEDURE

**3.1. Numerical Scheme** The discretized form of Equation (10) reads as:

$$A_{ij} \frac{\partial Q_{ijk}}{\partial t} = \left[ \sum_{m=1}^4 ((F_{ijk} - R_{ijk}) \Delta y - (G_{ijk} - S_{ijk}) \Delta x) - A_{ij} H_{ijk} \right]_m, k = 1, 2, 3, 4 \quad (5)$$

For time discretization, one can use backward method. So [22]

$$\frac{\partial Q_{ijk}}{\partial t} = \frac{Q_{ijk}^n - Q_{ijk}^{n-1}}{\Delta t} = \frac{1}{A_{ij}} \left[ \sum_{m=1}^4 ((F_{ijk} - R_{ijk}) \Delta y - (G_{ijk} - S_{ijk}) \Delta x) - A_{ij} H_{ijk} \right]^{n-1}, \quad (6)$$

$$k = 1, 2, 3, 4 \Rightarrow Q^n = \Delta t * \Psi(Q^{n-1}) + Q^{n-1}$$

where  $\Psi(Q^{n-1})$  is function of the velocities, the pressure, and the temperature in the last step. In this paper, for time discretization, a fifth-order Runge-Kutta is utilized which reads [23] as:

$$\Phi^{(0)} = Q^{n-1}, \Phi^{(p)} = \alpha_p \Delta t * \Psi(\Phi^{p-1}) + \Phi^{p-1}, \quad (7)$$

$$\alpha_p = \frac{1}{4}, \frac{1}{6}, \frac{3}{8}, \frac{1}{2}, 1, p = 1, 2, \dots, 5, Q^{(n)} = \Phi^{(5)}$$

To calculate the convective fluxes, the characteristic scheme is used [4]. The flux averaging method is numerically unstable under various conditions. Therefore, the forth-order damping term is used as [22]:

$$D = -\varepsilon (\Delta x)^4 \frac{\partial^4 u}{\partial x^4} = -\varepsilon (u_{i-2} - 4u_{i-1} + 6u_i - 4u_{i+1} + u_{i+2}). \quad (8)$$

where ‘D’ is the forth-order damping term and ‘ε’ damping coefficient. This term is added explicitly to the right hand side of Equaion (8). A negative sign is needed to produce positive dissipation. The viscous fluxes demand the computation of derivatives at the cell faces. For this purpose, the following procedure on the secondary cell is done (the green theorem is used again to convert double integral to line integral). The secondary cell is displayed in Figure 1.

$$\frac{\partial \eta}{\partial x} \Big|_{AB} = \frac{1}{S} \iint_S \frac{\partial \eta}{\partial x} ds = \frac{1}{S} \oint \eta dy = \frac{1}{S} \sum_{k=1}^4 \eta \Delta y_k, \eta = u, v, T. \quad (9)$$

In the above equation, k=1 to 4 are corresponding to the sides of the secondary cells. Now, the velocities and the temperature on the sides of the secondary cells must be determined. The corresponding variables are found by averaging. For example, values on first side are calculated by:

$$\eta_{k=1} = 0.5 * (\eta_A + \eta_{i,j}) = 0.5 * [0.25 * (\eta_{i,j} + \eta_{i,j+1} + \eta_{i+1,j} + \eta_{i+1,j+1}) + \eta_{i,j}]. \quad (10)$$

Nusselt number is calculated by:

$$Nu = \frac{\partial T}{\partial y} = \frac{T_{i,2} - T_{i,1}}{y_{i,2} - y_{i,1}} \quad (11)$$

To obtain the mean Nusselt number, this procedure is done.

$$\overline{Nu} = \int_0^1 Nu dx = \frac{1}{m} \sum_{i=1}^m Nu_i \quad (12)$$

**3.2. Boundary Conditions and Convergence History** No-slip condition is applied to determine the velocities and the temperature at the solid boundaries. The pressure is extrapolated from the interior domain as [22]:

$$p_s = 1.5p_{i,1} - 0.5p_{i,2} \quad (13)$$

For the velocities, the boundary conditions are  $u_{up}=1$ ,  $u_{down}=0$ ,  $u_{left}=0$ ,  $u_{right}=0$ . According to the given boundary conditions, the upper wall moves with constant velocity and others are motionless. The first thermal boundary conditions are:

$$T_{Up} = \sin(\pi x), T_{Down} = 0, T_{left} = 0, T_{Right} = \sin(\pi y). \quad (14)$$

Above equations show that the down and the left walls are cold. The maximum temperature of the right and the upper walls is in the middle points of the walls. The temperature of the right and the upper walls decrease sinusoidally from the middle point to the sides. Error at every steps is calculated by Equation (15) in this work [22].

$$Error = \sqrt{\frac{\sum \sum (v_{i,j}^{n+1} - v_{i,j}^n)^2}{N * M}} \quad (15)$$

**4. RESULTS AND DISCUSSION**

Extensive runs of FORTRAN code have been performed to reveal the effects of time-step since our first aim is to obtain time marching solutions, which are steady. However, unsteady solution can be obtained by time marching after passing the primary convergence process and damping the initially produced noises. Convergence history is calculated from Equation (15) and results are displayed in Figure 2. Convergence happens later for large Grashof numbers.

In the first part of this work, forced convection is simulated for various Prandtl numbers, Re=100, and Gr=0. Isotherms are shown in 0 at different Prandtl numbers at Re=100 and Gr=0. For large Prandtl numbers, thermal boundary layers affects the small area and for small Prandtl numbers. Thermal boundary layers affects the large area of domain according to Figure 3.

Nusselt number for upper and down walls is displayed in Figure 4 and Figure 5 for different Prandtl numbers at Re=100 and Gr=0. Nusselt number is higher for large Prandtl numbers. Thermal conductivity is low for large Prandtl and Nusselt numbers. Nusselt number for upper wall is more than Nusselt number for down wall. Upper wall moves with constant velocity and so the

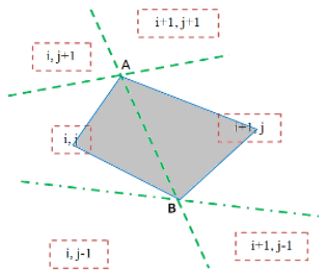


**Figure 1.** Stencil for discretization of viscous fluxes [5]

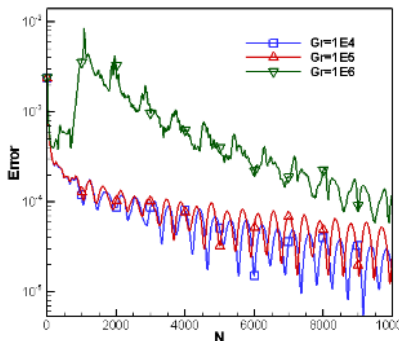


**Figure 2.** Convergence history at Re=100 and Pr=0.1

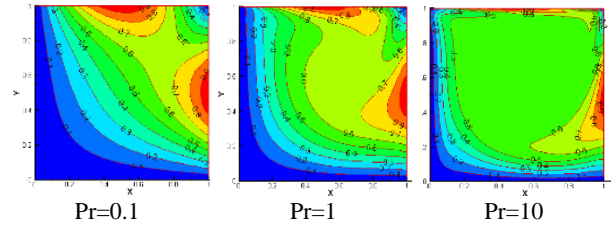


**Figure 3.** Isotherms in the different Prandtl numbers at Re=100, Gr=0

boundary layer is formed on the upper wall and then velocity of fluid is more inside the boundary layer (near the upper wall). High velocity near the upper wall increases the heat transfer from upper wall to the fluid and then Nusselt number is high in this region. In some parts of the upper wall, the Nusselt number is negative. This means that heat transfer direction is from fluid to the wall in this part. In other words, this shows that the temperature of fluid is greater than that of the wall. These are due to the given thermal boundary conditions. Accordingly, the thermal boundary conditions temperature of upper and right walls changes sinusoidally and the temperature of these walls is high in the middle parts and low in the side areas. The Nusselt number is low in the left part of upper wall due to low thickness of the thermal boundary layer in that part.

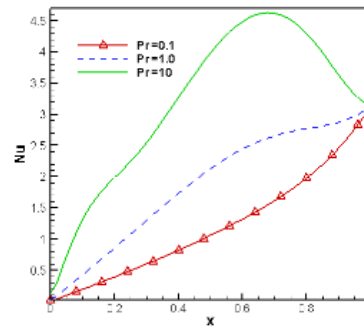


**Figure 4.** Nusselt number variation for down wall at different Prandtl number, Gr=0, Re= 100

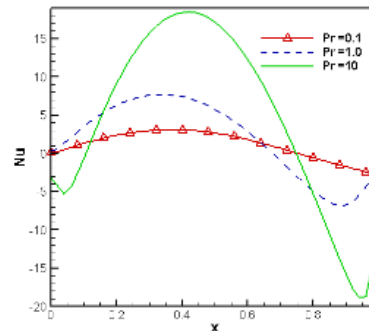


**Figure 5.** Nusselt number for upper wall in the different Prandtl number at Gr=0, Re= 100

Nevertheless, in the down wall, Nusselt number variation is complex and Nusselt number is maximum in the middle part of down wall. Mean Nusselt number is shown in Table 1. The mean Nusselt number for upper wall is more than that for down wall for the reason mentioned above. Also, mean Nusselt number is high at large Prandtl numbers similar to Nusselt number. Therefore, mean Nusselt number is higher for coolant liquid in comparison with molten liquids. Molten liquids have high conductivity coefficient, hence, their Prandtl numbers is low and their Nusselt numbers in thermos-flow is high.

In this section, the influence of Grashof number on flow parameters is surveyed. Streamlines in the different Grashof numbers at Re=300 and Pr=1 is shown in Figure 6. In low Grashof numbers, one main vortex and two small vortices are formed in the cavity. The small vortices grow upper in the larger Grashof numbers. These vortices join each other and make a big vortex in the down part of the cavity in higher Grashof numbers. As the Grashof number rises, the free convection flow within closed domain tends to become stratified. Free convection is stronger at high Grashof numbers. It forces fluid to move. Free and forced convections are combined with each other and make new streamlines.

Isotherms in the different Grashof numbers at Re=300 and Pr=1 is displayed in Figure 7. Forced convection

**TABLE 1.** Mean Nusselt number for upper and down walls at Gr=0, Re= 100

	Pr=0.1	Pr=1	Pr=10
Down wall	1.202	1.871	3.158
Up wall	1.096	1.901	4.313

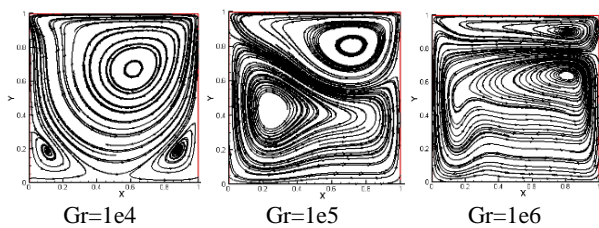


**Figure 6.** Stream lines in different Grashof numbers at Re=300, Pr=1

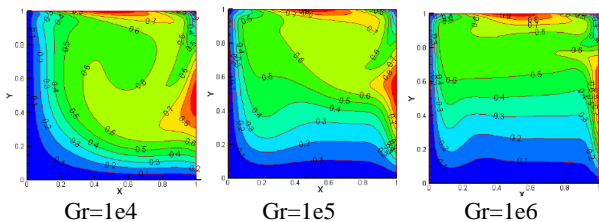


**Figure 7.** Isotherms in different Grashof numbers at Re=300, Pr=1

dominates in small Grashof numbers and isotherms in small Grashof numbers is similar to isotherms in forced convections. Isotherms change in large Grashof numbers. The Nusselt number for the upper and down walls is calculated and shown in Figures 8 and 9 for different Grashof numbers at Re=300 and Pr=1. These figures are similar to Figures 4 and 5. Nusselt number for upper wall is higher than that for down wall in both. The effect of Prandtl number on Nusselt number is more than that of Grashof number on Nusselt number according to these figures. Mean Nusselt number for upper and down walls at Gr=0, Re= 100 is displayed in Table 2. The mean Nusselt number is low in high Grashof numbers. Grid independency is shown in Figure 10. Simulation is done in three different grids, namely 30×30, 50×50 and 80×80 cells for the first, second and third simulations, respectively.

In the final part of this paper, the results are validated by those of Iwatsu et al. [24] by changing thermal boundary conditions in the written code and are in Figure 11. The small difference between the two results is normal and due to the different specifications of Iwatsu et al. and our schemes.

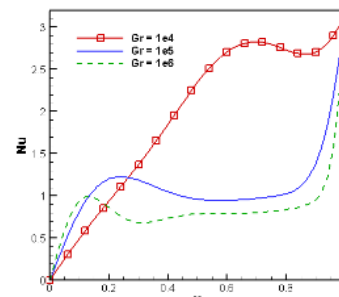


**Figure 8.** Nusselt number for down wall in different Grashof numbers at Pr=1, Re= 300

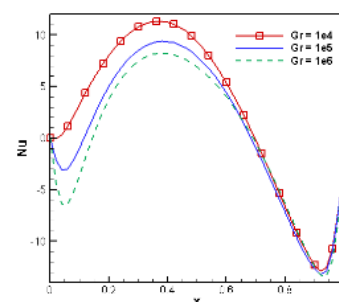


**Figure 9.** Nusselt number for upper wall in different Grashof numbers at Pr=1, Re= 300

**TABLE 2.** Mean Nusselt number for upper and down walls at Gr=0, Re= 100

	Gr=1e4	Gr=1e5	Gr=1e6
Down wall	1.95	1.11	0.88
Up wall	2.42	0.80	0.06

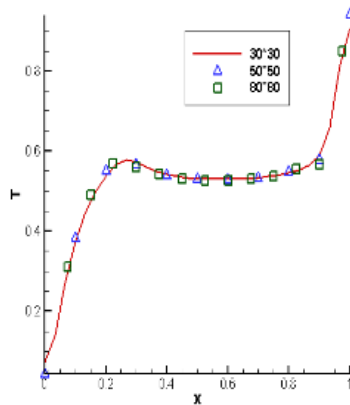


Figure 10. Grid independency at  $Re=500$ ,  $Pr=2$ ,  $Gr=1000$

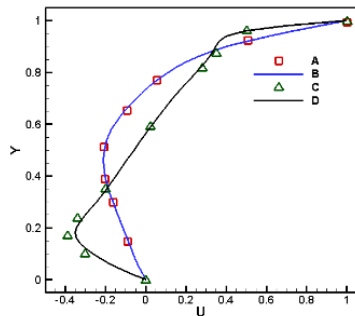


Figure 11. Comparing our results with Iwatsu et al. [24] results. A) Iwatsu et al. results for  $Re=100$ , B) Our results for  $Re=100$ , C) Iwatsu results for  $Re=1000$ , D) Our results for  $Re=1000$

## 5. CONCLUSION

In this paper, free and forced convections in cavity are simulated by a characteristic based method. Simulations are done for the Prandtl numbers varying from 0.1 to 10, the Grashof numbers between 0 and  $10^6$  and Reynolds numbers between 100 and 1000. The results show that the Nusselt number is high for water and coolant liquid in comparison with air and molten liquids. The numbers and size of vortices in the cavity depend on Grashof number. As the Grashof number rises, the natural convection flow within closed domain tends to become stratified. Also, for low-viscosity fluids, rising the Nu demonstrate higher changes in flow pattern than the high-viscosity ones.

## 6. REFERENCES

- Moallemi, M.K. and Jang, K. S., "Prandtl number effects on laminar mixed convection heat transfer in a lid-driven cavity", *International Journal of Heat and Mass Transfer*, Vol. 35, No. 8, (1992), 1881–1892.
- Oztop, H.F. and Dagtekin, I., "Mixed convection in two-sided lid-driven differentially heated square cavity", *International Journal of Heat and Mass Transfer*, Vol. 47, No. 8–9, (2004), 1761–1769.
- Sharif, M. A. R., "Laminar mixed convection in shallow inclined driven cavities with hot moving lid on top and cooled from bottom", *Applied Thermal Engineering*, Vol. 27, No. 5–6, (2007), 1036–1042.
- Adibi, T. and Razavi, S. E., "A new characteristic approach for incompressible thermo-flow in Cartesian and non-Cartesian grids", *International Journal for Numerical Methods in Fluids*, Vol. 79, No. 8, (2015), 371–393.
- Razavi, S.E. and Adibi, T., "A Novel Multidimensional Characteristic Modeling of Incompressible Convective Heat Transfer", *Journal of Applied Fluid Mechanics*, Vol. 9, No. 3, (2016), 1135–1146.
- Christopher, D. M., "Numerical prediction of natural convection in a tall enclosure", *International Journal for Numerical Methods in Fluids*, Vol. 40, No. 8, (2002), 1039–1044.
- El-Refaei, M.M., Elsayed, M.M., Al-Najem, N.M. and Noor, A. A., "Natural convection in partially cooled tilted cavities", *International Journal for Numerical Methods in Fluids*, Vol. 28, No. 3, (1998), 477–499.
- Padilla, E.L.M., Lourenço, M.A. and Silveira-Neto, A., "Natural convection inside cubical cavities: numerical solutions with two boundary conditions", *Journal of the Brazilian Society of Mechanical Sciences and Engineering*, Vol. 35, No. 3, (2013), 275–283.
- Selimefendigil, F., "Numerical analysis and identification of mixed convection in pulsating flow in a square cavity with two ventilation ports in the presence of a heating block", *Journal of the Brazilian Society of Mechanical Sciences and Engineering*, Vol. 35, No. 3, (2013), 265–273.
- Labsi, N., Benkahla, Y.K., Boutra, A. and Titouah, M., "Convection heat transfer inside a lid-driven cavity filled with a shear-thinning Herschel–Bulkley fluid", *Journal of the Brazilian Society of Mechanical Sciences and Engineering*, Vol. 40, No. 123, (2018), 1–25.
- Bousset, F., Lyubimov, D.V. and Sedel’Nikov, G. A., "Three-dimensional convection regimes in a cubical cavity", *Fluid Dynamics*, Vol. 43, No. 1, (2008), 1–8.
- Gershuni, G.Z., Zhukhovitskii, E.M. and Yurkov, Y. S., "Vibrational thermal convection in a rectangular cavity", *Fluid Dynamics*, Vol. 17, No. 4, (1982), 565–569.
- Alonso, A. and Batiste, O., "Onset of oscillatory binary fluid convection in three-dimensional cells", *Theoretical and Computational Fluid Dynamics*, Vol. 18, No. 2–4, (2004), 239–249.
- Boeck, T., "Low-Prandtl-number Bénard-Marangoni convection in a vertical magnetic field", *Theoretical and Computational Fluid Dynamics*, Vol. 23, No. 6, (2009), 509–524.
- Jami, M., Mezrhab, A. and Naji, H., "Numerical study of natural convection in a square cavity containing a cylinder using the lattice Boltzmann method", *Engineering Computations*, Vol. 25, No. 5, (2008), 480–489.
- Armfield, S. and Schultz, A., "Unsteady natural convection in tall side-heated cavities", *International Journal for Numerical Methods in Fluids*, Vol. 40, No. 8, (2002), 1009–1018.
- Raji, A. and Hasnaoui, M., "Combined mixed convection and radiation in ventilated cavities", *Engineering Computations*, Vol. 18, No. 7, (2001), 922–949.
- Mondal, P.K. and Mukherjee, S., "An Analytical Approach to the Effect of Viscous Dissipation on Shear-Driven Flow between two parallel plates with Constant Heat Flux Boundary Conditions",

- International Journal of Engineering-Transactions B: Applications*, Vol. 26, No. 5, (2013), 533–542.
19. Gandjalikhan, N., Shahsavari, A. and Moghimi, M. A., “Analysis of combined conduction and radiation heat transfer in a rectangular furnace including two heat sources”, *International Journal of Engineering-Transactions A: Basics*, Vol. 21, No. 5, (2012), 65–70.
  20. Mazaheri, K., Banai, A. and Seyed-Reyhani, S. A., “Adaptive Unstructured Grid Generation Scheme for Solution of the Heat Equation”, *International Journal of Engineering-Transactions A: Basics*, Vol. 13, No. 4, (2000), 43–54.
  21. Incropera, F.P., Lavine, A.S., Bergman, T.L. and Dewitt, D.P., *Introduction to heat transfer*, John Wiley & Sons, (2007).
  22. Anderson, J.D. and Wendt, J., *Computational fluid dynamics* (Vol. 206), New York: McGraw-Hill, (1995).
  23. Adibi, T., “Three-dimensional characteristic approach for incompressible thermo-flows and influence of artificial compressibility parameter”, *Journal of Computational & Applied Research in Mechanical Engineering (JCARME)*, Vol. 8, No. 2, (2019), 223–234.
  24. Iwatsu, R., Hyun, J.M. and Kuwahara, K., “Mixed convection in a driven cavity with a stable vertical temperature gradient”, *International Journal of Heat and Mass Transfer*, Vol. 36, No. 6, (1993), 1601–1608.

## A Characteristic-based Solution of Forced and Free Convection in Closed Domains with Emphasis on Various Fluids

T. Adibi<sup>a</sup>, O. Adibi<sup>b</sup>, S. E. Razavi<sup>c</sup>

<sup>a</sup> Department of Mechanical Engineering, University of Bonab, Bonab, Iran

<sup>b</sup> Department of Mechanical Engineering, Sharif University of Technology, Tehran, Iran

<sup>c</sup> Department of Mechanical Engineering, University of Tabriz, Tabriz, Iran

### P A P E R I N F O

### چکیده

#### Paper history:

Received 23 August 2019

Received in revised form 12 September 2019

Accepted 13 September 2019

#### Keywords:

complex boundary conditions  
convection

Grashof number  
numerical method

Nusselt number  
Prandtl number

در این مقاله جابجایی آزاد و اجباری در شرایط مرزی پیچیده شبیه‌سازی شده‌اند. دما در دیواره‌ی بالا و راست به‌طور سینوسی تغییر می‌کند و در بقیه‌ی دیواره‌ها صفر است. تاثیر عدد گراشف و پرانتل روی الگوی جریان بررسی شده است. مواد مختلفی از جمله فلزات مذاب و مایع مبرد مورد مطالعه قرار گرفته است. کدی در نرم‌افزار فرترن نوشته شد و گسسته-سازی عددی با روش ران کوتا و جملات هم‌رفت با روش مشخصه‌ی پایه محاسبه شد. جریان، تراکم‌ناپذیر دو بعدی و لایه‌ای فرض شده است. نتایج نشان داد با افزایش عدد گراشف، عدد ناسلت زیاد می‌شود. اثر عدد گراشف روی عدد ناسلت صفحه‌ی بالا بیشتر از صفحه‌ی پایین است، اما اثر عدد پرانتل روی عدد ناسلت هر دو صفحه تقریباً یکسان است.

doi: 10.5829/ije.2019.32.11b.20